The Journal of Chemical Physics

RESEARCH ARTICLE | MARCH 09 2026

Random walks and the electronic structure of graphene

Nino Bašić ; Patrick W. Fowler ; Barry T. Pickup ; Primož Potočnik

J. Chem. Phys. 164, 104103 (2026)
https://doi.org/10.1063/5.0319282

The Journal of Chemical Physics ARTICLE pubs.aip.org/aip/jcp

Random walks and the electronic structure of graphene

Cite as: J. Chem. Phys. 164, 104103 (2026); doi: 10.1063/5.0319282
Submitted: 23 December 2025 • Accepted: 24 February 2026 •
Published Online: 9 March 2026

Nino Bašić,[1,2,3,a] Patrick W. Fowler,[4,b] Barry T. Pickup,[4,c] and Primož Potočnik[3,5,d]

AFFILIATIONS

[1] FAMNIT, University of Primorska, Koper, Slovenia
[2] IAM, University of Primorska, Koper, Slovenia
[3] Institute of Mathematics, Physics and Mechanics, Ljubljana, Slovenia
[4] Chemistry, School of Mathematics and Physical Sciences, University of Sheffield, Sheffield S3 7HF, United Kingdom
[5] Faculty of Mathematics and Physics, University of Ljubljana, Ljubljana, Slovenia

[a] Electronic mail: nino.basic@famnit.upr.si
[b] Electronic mail: P.W.Fowler@sheffield.ac.uk
[c] Author to whom correspondence should be addressed: B.T.Pickup@sheffield.ac.uk
[d] Electronic mail: primoz.potocnik@fmf.uni-lj.si

ABSTRACT

Results from the mathematical literature on random walks reveal a closed-form analytical expression for the π-energy and bond number of graphene in the simplest tight-binding model and its Hartree–Fock Hubbard extension. Closed-form expressions follow for all π spectral moments of graphene. Bond numbers of carbon and boron nitride (BN) zigzag nanotubes are found as finite sums, with graphene and hexagonal boron nitride sheets as asymptotes.

I. INTRODUCTION

In this paper, we show how some recent progress in the mathematical literature on closed-form expressions for random walk integrals[1,2] has implications for a range of classic models of electronic structure. The central result is for the basic quantity in the tight-binding treatment of graphene (the π binding energy) and has consequences for the limiting behavior of a variety of chemical systems described with a two-atom unit cell. These include binary heteronuclear analogs of graphene, such as hexagonal boron nitride (hBN), nanotubes, and nanotori derived from the sheet materials. Furthermore, the tight-binding Hubbard model in the Hartree–Fock limit for each of these systems follows by reinterpretation of the hBN eigenvalue equations. Implications for two-dimensional models are derived from consideration of closed-form results for the average distance reached by a random walk of three steps of unit length in the plane.[1,2] Walks of two and four steps give related results for one- and three-dimensional systems, such as polyacetylene and diamond/zinc blende lattices.

II. BACKGROUND

Calculation of the electronic structure of single-sheet graphite was an early triumph of tight-binding band theory and gave a well-known formula for the π binding energy per atom,[3]

$$E_\pi = \frac{|t|}{4\pi^2} \int_{-\pi}^{\pi} \int_{-\pi}^{\pi} f(\theta_1, \theta_2)\, d\theta_1 d\theta_2, \tag{1}$$

where

$$f(\theta_1, \theta_2) = \{3 + 2\cos\theta_1 + 2\cos\theta_2 + 2\cos(\theta_1 - \theta_2)\}^{1/2} \tag{2}$$

and t is the hopping parameter (negative in the convention used in the chemical literature).

In the qualitative theory of finite carbon π-systems, π charges and bond orders are defined in terms of the eigenvectors of the adjacency matrix of the unweighted graph that represents the molecule. The π-bond order for the pair, rs, is

$$p^{\pi}_{rs} = \sum_{k} n_k c_{rk} c^{*}_{sk}, \tag{3}$$

where n_k is the occupation number of the molecular orbital and c_{rk} is the entry on the center r for eigenvector k. The diagonal term, $p^{\pi}_{rr} = q_r$, is the charge on the atom. The π bond number of the center r, denoted $\widetilde{N}_r$, is defined as the sum of the mobile bond orders of the incident bonds. The tilde indicates that the bond number is to be assigned its maximum value for the graph, which is achieved for the "natural" electron configuration, defined by $n_k = 2, 1, 0$, for positive, zero, and negative eigenvalues (bonding, nonbonding, and antibonding), respectively. For infinite systems, the sums over finite sets of states transmute into sums over bands, each integrated over the Brillouin zone. For graphene, the π bond number is independent of the label r and denoted by $\widetilde{N}(g)$, obtained by dividing the binding energy E_π per atom by the unsigned hopping parameter.

Bond number measures the contribution of an unsaturated center to overall stability[4] and is an indicator of reactivity toward homolytic attack (see a detailed discussion in Ref. 5). For any π system, $\widetilde{N}_r \le \sqrt{d_r}$, where d_r is the number of carbon neighbors of center r, with the bound $\sqrt{3}$ reached only by the central atom of trimethylenemethane.[6] The value of $\widetilde{N}(g)$ lies significantly below this limit.

III. GRAPHENE

Graphene has two atoms in its unit cell, as illustrated in Fig. 1. We concentrate on the π-electron structure, as described in a minimal basis set of one $2p_z$ orbital per atom. We transform to a basis of Bloch orbitals constructed from this to reflect the translational symmetry since the Abelian translational group then allows us to split the adjacency matrix into non-interacting 2×2 blocks, each labeled by the two-dimensional wavevector, $\boldsymbol{k}$, which describes the bands. In this basis, the off-diagonal matrix element in the block is

$$A_{12}(\boldsymbol{k}) = t\left(1 + e^{i\boldsymbol{k}\cdot\boldsymbol{R}_{12'}} + e^{i\boldsymbol{k}\cdot\boldsymbol{R}_{12''}}\right), \tag{4}$$

where $\boldsymbol{R}_{rs}$ is the distance vector from atom r to s. For our purposes, it is sufficient to replace the scalar products in the exponentials by simple angles, so that the secular equation blocks become

$$\begin{pmatrix} -\epsilon/t & 1 + e^{i\theta_1} + e^{i\theta_2} \\ 1 + e^{-i\theta_1} + e^{-i\theta_2} & -\epsilon/t \end{pmatrix}\begin{pmatrix} c_a \\ c_b \end{pmatrix} = \begin{pmatrix} 0 \\ 0 \end{pmatrix}, \tag{5}$$

leading to the eigenvalues for the two bands,

$$\epsilon_{\pm}(\theta_1, \theta_2) = \pm t|1 + e^{i\theta_1} + e^{i\theta_2}| = \pm t f(\theta_1, \theta_2), \tag{6}$$

with $f(\theta_1, \theta_2)$ as in Eq. (2). The π-binding energy per atom and, hence, $\widetilde{N}(g)$ follow by integration of the occupied band over the Brillouin zone.

Estimation of the graphene π bond number $\widetilde{N}(g)$ has a venerable history. As early as 1934, Wheland[7] reported a result implying $\widetilde{N}(g) \approx 1.58$, but without giving details of how it was calculated. Bradburn *et al.*[8] calculated $\widetilde{N}(g)$ by extrapolation of finite "crystallites" (H-terminated nanographenes) to give a value of 1.5761 (in the usual first approximation of zero overlap between p_π-orbitals on adjacent carbon centers). Coulson and Taylor[9] considered periodicity explicitly and extrapolated Bloch wavefunctions with toroidal boundary conditions to write the graphene limit as

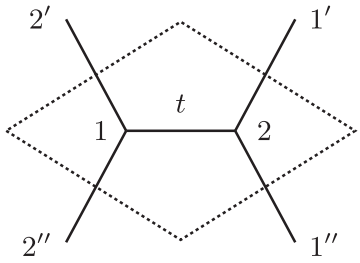

FIG. 1. Unit cell for graphene. Atom 1 is bonded to atom 2 within the cell and to copies of atom 2 in the neighboring cells above left (atom 2′) and below left (atom 2″).

$$\widetilde{N}(g) = \frac{4}{\pi^2}\int_0^{\pi/2} E(k)(1 + 2\cos\theta_1)\, d\theta_1, \tag{7}$$

where

$$E(k) = \int_0^{\pi/2} (1 - k^2 \sin^2\theta_2)^{1/2}\, d\theta_2 \tag{8}$$

is a complete elliptic integral of the second kind and its modulus, k, satisfies $k^2 = 8\cos\theta_1/(1 + 2\cos\theta_1)^2$. The authors of Ref. 9 did not evaluate Eq. (7) analytically, but their numerical integration gave $\widetilde{N}(g) \approx 1.576$, in the case of zero overlap. This agrees with the value obtained earlier[10] by extrapolation of numerical results for finite toroidal nanographenes. Recent numerical integration[6] of Eq. (7) to higher precision gave 1.574 597, i.e., ≈ 1.575.

IV. RANDOM WALKS IN THE PLANE

It turns out that the incremental approach toward the exact value can be circumvented since a closed formula for $\widetilde{N}(g)$ has been hiding in the mathematical literature under another guise. The work in question relates to properties of the random walk. This problem was first given prominence by Pearson, whose 1905 Letter to Nature[11] asked for the probability that a walk of n randomly directed steps of equal length reaches a given distance from the origin. His next letter[12] noted that Mr. Bennett knew that the solution for $n = 3$ involved elliptic integrals.

Here, we consider a three-step walk in the plane, where each step has unit length, and a turn through a randomly chosen angle is made before each new step, as shown in Fig. 2,

$$\begin{aligned} a_1(\theta_1, \theta_2) &= 1, \quad a_2(\theta_1, \theta_2) = \sqrt{2 + 2\cos\theta_1}, \\ a_3(\theta_1, \theta_2) &= \sqrt{3 + 2\cos\theta_1 + 2\cos\theta_2 + 2\cos(\theta_1 - \theta_2)}. \end{aligned} \tag{9}$$

The average distance from the origin over many walks is

$$\langle R \rangle = \frac{1}{4\pi^2}\int_{-\pi}^{\pi} d\theta_1 \int_{-\pi}^{\pi} d\theta_2\, a_3(\theta_1, \theta_2), \tag{10}$$

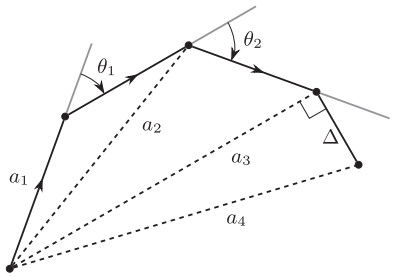

FIG. 2. Three-step random walk in the plane. Each step has a unit length. After steps 1 and 2, the walk turns through a randomly chosen angle. Successive distances from the origin are a_1, a_2, and a_3. The shifted walk that is to be used in discussion of hBN lattices adds a hop of Δ at right angles to the third distance vector, to reach final distance $a_4 = \sqrt{\Delta^2 + a_3^2}$.

where the angles are considered as uniformly distributed random variables taking values in the interval $[0, 2\pi]$. We can use complex arithmetic to take the square root implicit in a_3, giving

$$\langle R \rangle = \frac{1}{4\pi^2} \int_{-\pi}^{\pi} d\theta_1 \int_{-\pi}^{\pi} d\theta_2 \left| 1 + e^{i\theta_1} + e^{i\theta_2} \right| = W_3(1). \tag{11}$$

Here, the symbol $W_3(1)$ denotes a specific case of the general expression[1,2] for the average of the sth power of the distance for a random walk of n unit steps,

$$W_n(s) = \frac{1}{(2\pi)^n} \int_{-\pi}^{\pi} d\theta_1 \ldots \int_{-\pi}^{\pi} d\theta_n \left| 1 + \sum_{j=1}^{n-1} e^{i\theta j} \right|^s. \tag{12}$$

Comparison of Eqs. (1) and (11) gives

$$\widetilde{N}(\mathrm{g}) = W_3(1). \tag{13}$$

Borwein *et al.*[1,2] stated and proved a conjecture relating $W_3(s)$ to hypergeometric functions, from which they deduced several closed forms for $W_3(1)$, including

$$W_3(1) = \frac{2^{1/3}}{\pi^4} \frac{3}{16} \Gamma^6\left(\frac{1}{3}\right) + \frac{2^{2/3}}{\pi^4} \frac{27}{4} \Gamma^6\left(\frac{2}{3}\right), \tag{14}$$

where Γ is the Gamma function,[13] and in fact, as $\Gamma(2/3) = 2\pi/(\sqrt{3}\,\Gamma(1/3))$, only one evaluation of the special function is required. The quantity $W_3(1)$ can be calculated with high precision (see the evaluation by David Bailey reported in Ref. 1).

For the present discussion, the significance of Eqs. (13) and (14) is that there is finally a closed-form solution to the chemical physics problem that Coulson's group set for themselves in the 1940s. The key to progress was to return to the full two-dimensional form of the integral and enable the direct connection to $W_3(1)$. Furthermore, recursion relations and exact results for $W_3(s)$ proved in Ref. 2 provide expressions for all π spectral moments[14] of graphene.

V. HEXAGONAL BORON NITRIDE

Graphene can also be treated as the formal limit of a heteroatomic layer material in which electronegativity differences have been allowed to tend to zero. One such material is hexagonal boron nitride,[15] where the B and N atoms have electronegativities that bracket the carbon value. Here, it proves useful to go back to considering the two integration steps separately.

A unified picture of the π-bands in hBN and graphene is constructed by defining vertex weights [diagonal entries in the adjacency matrix of Eq. (5)], assigned values at and bt for B and N (sites 1 and 2 in Fig. 1), respectively. In this picture, the vertex π-energy[14] is

$$E_c^\pi = t\left(N_c^\pi + cq_c^\pi\right), \qquad \text{for } c = a, b. \tag{15}$$

The band energies for the hBN sheet are then

$$\epsilon_\pm = t\left[\frac{1}{2}(a+b) \pm D\right], \tag{16}$$

where the discriminant is given by

$$D^2 = \Delta^2 + f(\theta_1, \theta_2)^2 \tag{17}$$

and the bandgap parameter is $\Delta = \frac{1}{2}|a - b|$.

We now define ancillary quantities, X_E and X_K, in terms of complete elliptic integrals as

$$\begin{aligned} X_E &= \frac{4}{\pi^2} \int_0^{\pi/2} E(k)\left(\Delta^2 + (1 + 2\cos\theta)^2\right)^{\frac{1}{2}} d\theta, \\ X_K &= \frac{4}{\pi^2} \int_0^{\pi/2} K(k)\left(\Delta^2 + (1 + 2\cos\theta)^2\right)^{-\frac{1}{2}} d\theta, \end{aligned} \tag{18}$$

with the usual angular dependence of k. With these definitions, charges on centers in the unit cell are

$$q_a^\pi = 1 + \frac{1}{2}(a-b)X_K, \quad q_b^\pi = 1 - \frac{1}{2}(a-b)X_K, \tag{19}$$

and the π bond numbers are

$$\widetilde{N}_a^\pi = \widetilde{N}_b^\pi = X_E - \Delta^2 X_K, \tag{20}$$

with $\widetilde{N}_a^\pi = \widetilde{N}_b^\pi = \widetilde{N}(\mathrm{hBN})$ being the unique bond number of the hBN sheet. The two distinct vertex π-energies are

$$\begin{aligned} E_a^\pi/t &= a + X_E + \frac{1}{4}(a^2 - b^2)X_K, \\ E_b^\pi/t &= b + X_E - \frac{1}{4}(a^2 - b^2)X_K. \end{aligned} \tag{21}$$

Note that the sum of the two gives the total energy per unit cell associated with the filled band.

When $\Delta = 0$, all terms involving X_K vanish, to give the correct graphene limits for all quantities.

Numerical integration of Eq. (18) gives $\widetilde{N}(\mathrm{hBN}) = 1.574\,597$, $1.491\,902$, $1.334\,431$, and $1.174\,106$ for $\Delta = 0$, $1/2$, 1, and $3/2$. Further analysis shows that although no Taylor series expansion about $\Delta = 0$ exists for $\widetilde{N}(\mathrm{hBN})$, the expression

$$\widetilde{N}(\mathrm{hBN}) = W_3(1) - \frac{1}{2}W_3(-1)\Delta^2 + \frac{4}{3\sqrt{3}\pi}\Delta^3 + o(\Delta^3) \tag{22}$$

with[2]

$$W_3(-1) = \frac{2^{1/3}}{\pi^4}\frac{3}{16}\Gamma^6\left(\frac{1}{3}\right) \tag{23}$$

gives a cubic approximation accurate to 3% for the chemically relevant range $0 \le \Delta \le 1$.

In the limit of large Δ, the bond number goes to zero as a series in odd powers of $1/\Delta$,

$$\begin{aligned}\widetilde{N}(\mathrm{hBN}) &= \frac{1}{\Delta}\sum_{j=0}^{\infty}\frac{(-1)^j(2j)!}{2^{2j}j!^2}W_3(2j+2)\frac{1}{\Delta^{2j}}\\ &= 3\Delta^{-1} - \frac{15}{2}\Delta^{-3} + O(\Delta^{-5}).\end{aligned} \tag{24}$$

The moments $W_3(s)$ with even s are integers (see the sequence https://oeis.org/A002893 in the OEIS[16]).

Figure 3 shows that the cubic approximation is useful for $\Delta < 1$. The asymptotic expansion converges for $\Delta > 3$.

The expression for energies of the π-bands of the hBN sheet Eq. (16) can also be interpreted in terms of walks, if we are prepared to augment the usual three-step random walk with an extra hop. As shown in Fig. 2, the hop takes a direction perpendicular to the position vector after the third step and for our application, it is taken to be of length Δ, which is equal to the bandgap parameter. After this fourth move, the walker is at distance $a_4 = \sqrt{\Delta^2 + a_3^2}$ from the origin, i.e., at distance D, as defined by the square in Eq. (17).

VI. THE HUBBARD MODEL

The Hubbard model was developed to account for strong electron–electron interactions in solids with narrow d-bands.[17–19] A two-electron potential,

$$V = Ut\sum_{\mathrm{p}}\hat{n}_{\mathrm{p}\alpha}\hat{n}_{\mathrm{p}\beta}, \tag{25}$$

is added to the one-electron Hamiltonian, where second quantized operators, $\hat{n}_{\mathrm{p}\sigma}$, count electrons on the center p with spin σ. The factor U measures the strength of the interaction in units of the hopping parameter. In our parameterization, a negative U describes repulsive electron interactions. The Hubbard model can be solved exactly in only a few cases and the self-consistent Hartree–Fock (HF) approximation is often applied.

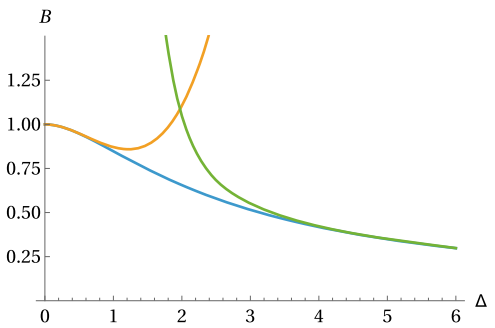

FIG. 3. Variation of bond number for hBN with bandgap Δ in the simplest tight-binding model. B is the ratio $\widetilde{N}(\mathrm{hBN})/\widetilde{N}(\mathrm{g})$. Plotting conventions for the curves are as follows: blue indicates numerical integration, orange represents the cubic approximation Eq. (22), and green represents the series expansion Eq. (24).

In the tight-binding context, the Fock matrix for closed shells[20] is an adjusted adjacency matrix,

$$F_{\mathrm{pq}} = A_{\mathrm{pq}} + \frac{1}{2}\delta_{\mathrm{pq}}Utq_p, \tag{26}$$

with vertex weights and the usual edge weights. The Fock matrix for Hubbard graphene is identical in form to that for hBN, with $a = Uq_a/2, b = Uq_b/2$.

To solve the HF Hubbard equations, we assume charges q_a and q_b, construct the resulting Fock matrix, use its eigenvectors to find new charges, and repeat to self-consistency. Symmetric tight-binding values, $q_a = q_b = 1$, give $\Delta = |a - b|/2 = 0$ and are already self-consistent. The band energies are identical, apart from a constant shift of $U/2$, to those for $U = 0$. Furthermore, the bond number for Hubbard graphene with negative U is identical to that for Hückel graphene with $U = 0$; i.e., it is equal to $W_3(1)$.

Are non-symmetric solutions to the HF Hubbard graphene equations possible? From Eq. (19),

$$q_a - q_b = (a - b)X_K = \frac{1}{2}(q_a - q_b)UX_K, \tag{27}$$

the self-consistency requirement is seen to be

$$\frac{1}{2}UX_K(\Delta^2) = 1, \tag{28}$$

where the argument of the function X_K is

$$\Delta^2 = \frac{1}{16}U^2(q_a - q_b)^2. \tag{29}$$

As X_K is positive for all finite Δ, self-consistency cannot be achieved for negative U.

However, for positive U, representing attraction, as used in phenomenological models of superconductivity, symmetry-broken solutions are possible. Trial calculations show solutions with $|q_a - q_b| > 0$ for U exceeding a critical value close to 2.3, in which charge asymmetry increases and bond number falls as U increases.

An analogous treatment for hBN incorporates both electronegativity difference and electron repulsion in one effective Δ parameter. Solutions with $q_a \neq q_b$ emerge naturally, as there is no symmetry exchanging the two sites. We note that our cubic approximation for $\widetilde{N}(\mathrm{hBN})$ in Eq. (22) exactly mirrors the numerical Eq. (26) of Ref. 21 for bond order per electron, which was derived for a Hubbard model of doped systems.

VII. NANOTUBES

We can also approach $\widetilde{N}(\mathrm{g})$ for graphene via the bond numbers of single-walled nanotubes for which the radius is allowed to grow without limit, or polyhex nanotori, where both radii of the torus are allowed to increase. For a given nanotube or polyhex nanotorus, all carbon atoms have equal bond number since the molecular graph is vertex-transitive.

Nanotubes are described by Hamada indices (n_1 and n_2), which specify the tube in terms of wrappings of the graphene sheet onto a

cylinder.[22,23] In general, where $n_1 \neq n_2 \neq 0$, the tube is chiral. Special cases $(n_1, 0)$ and (n_1, n_1) correspond to zigzag and armchair tubes, respectively. In the simplest tight binding model, metallic nanotubes are all those with $|n_1 - n_2| = 0 \bmod 3$ (leapfrog tubes).[24] In models that include s–p interaction, gaps open for the leapfrog zigzag and chiral tubes and they become semiconductors, but armchairs remain metallic.[25,26]

Nanotubes based on hBN are stable wide-gap insulators and give access to a different range of properties.[27–29] A unified picture of the π-bands in hBN- and carbon-based nanotubes can be constructed along the same lines as for the sheet materials. We now have translational and helical symmetries, which lead once more to factorization of the secular equation into 2×2 blocks. A nanotube with Hamada signature (n_1, n_2) has $\gcd(n_1, n_2)$ pairs of bands. As a generalization of the usual treatment for carbon nanotubes,[30,31] the band energies for a zigzag hBN tube with $n_1 = n, n_2 = 0$ are

$$E^{\pm}_{nq} = t\left[\frac{1}{2}(a+b) \pm D_{nq}\right], \quad \text{where } 0 \leq q \leq n-1, \tag{30}$$

with the discriminant given by

$$D^2_{nq} = \Delta^2 + (1 + 2\cos(\pi q/n))^2 - 8\cos(\pi q/n)\sin^2 x. \tag{31}$$

Charges on centers in the unit cell, bond number, and vertex energies are given by Eqs. (19)–(21),

$$\begin{aligned} X_E &= \frac{2}{\pi}\frac{1}{n}\sum_{q=0}^{n-1} F_{nq}E(k_{nq}), \\ X_K &= \frac{2}{\pi}\frac{1}{n}\sum_{q=0}^{n-1} F^{-1}_{nq}K(k_{nq}), \end{aligned} \tag{32}$$

with

$$F^2_{nq} = \Delta^2 + (1 + 2\cos(\pi q/n))^2 \tag{33}$$

and

$$k^2_{nq} = \frac{8\cos(\pi q/n)}{F^2_{nq}}. \tag{34}$$

The expressions for X_K and X_E are now short sums over occupied bands. As a consequence of helical symmetry, q plays the role of an angular momentum quantum number and contributions for bands with q and $\gcd(n_1, n_2) - q$ are degenerate.

Cognate expressions for armchair nanotubes are considerably more complicated; they involve three types of incomplete elliptic integrals, but still provide a finite sum of closed-form terms. For chiral nanotubes, it seems necessary to rely on numerical integration.

It has been noticed[6] that bond numbers for carbon nanotubes, calculated in the simplest tight-binding model, converge to the graphene limit from below for leapfrogs and otherwise from above. The finite sums in Eq. (32) suggest an explanation for this dichotomy: for zigzag tubes, band contributions per electron decrease with angular momentum, whereas the equivalent sums for armchairs show the opposite trend. Scatterplots for hBN tubes show blurring of this distinction, as bond numbers for leapfrog and non-leapfrog tubes appear on both sides of the asymptote for the sheet. For large Hamada parameters or bandgap, all points ultimately swarm onto the line for the corresponding sheet. Interestingly, the armchair hBN tubes, while still converging to it, lie strictly below the asymptote for all values of Δ. The compression of the scatterplot is consistent with observations[29] that properties of BN nanotubes depend only weakly on their Hamada parameters.

VIII. CONCLUSIONS

A central observation is that there is a one-to-one correspondence between the two angles that describe a walk of three equal steps in the plane and a point in the Brillouin zone in a band described by the tight-binding model of graphene. Graphene has two atoms per unit cell, and translational symmetry leads to the occurrence of sums of unimodular exponentials in the 2×2 blocks of the secular equations Eq. (5). These are identical in form to those that describe distances in the random walk problem. This simple observation has allowed exploitation of mathematical progress on that problem in order to comment on a variety of physical models of electronic structures of graphene and related systems.

It is clear that the same analogy also extends to one- and three-dimensional systems that can be described with two-atom unit cells. Thus, $W_2(1)$ and $W_4(1)$ give the bond numbers for undistorted polyacetylene and diamond,[32] respectively: $W_2(1)$ is exactly $4/\pi$ and $W_4(1)$ evaluates to 1.799 092 479 8 . . ..[1]

Similar parallels can be drawn for random-walk moments $W_n(s)$ with $s > 1$. Powers of the adjacency matrix count walks along edges of a graph, i.e., $(\mathbf{A}^s)_{pq}$ is the number of walks of length s from vertex p to vertex q, and in particular, diagonal entries count self-returning walks. The trace $\mathrm{Tr}(\boldsymbol{A}^s)$ is also the sum of the s-th powers of the eigenvalues. In tight-binding models of bipartite systems, the trace for even s is the expectation value of the s-th power of the Hamiltonian. For extended systems, the summation of discrete eigenvalues is replaced by Brillouin zone integrals over the band contributions. The implication for graphene is that $W_3(2j)$ has at least three roles. It is (i) the expected value of the $2j$-th power of the distance in the three step random walk problem, (ii) the number of self-returning walks of length $2j$ for the honeycomb lattice, and (iii) the $2j$-th spectral moment for graphene in the tight-binding model.

ACKNOWLEDGMENTS

This work was supported in part by the Slovenian Research Agency (Research Program P1-0294, Nino Bašić and Primož Potočnik).

AUTHOR DECLARATIONS

Conflict of Interest

The authors have no conflicts to disclose.

Author Contributions

All authors contributed equally to this work.

Nino Bašić: Conceptualization (equal); Formal analysis (equal); Investigation (equal); Methodology (equal); Writing – original draft

(equal); Writing – review & editing (equal). **Patrick W. Fowler**: Conceptualization (equal); Formal analysis (equal); Investigation (equal); Methodology (equal); Writing – original draft (equal); Writing – review & editing (equal). **Barry T. Pickup**: Conceptualization (equal); Formal analysis (equal); Investigation (equal); Methodology (equal); Writing – original draft (equal); Writing – review & editing (equal). **Primož Potočnik**: Conceptualization (equal); Formal analysis (equal); Investigation (equal); Methodology (equal); Writing – original draft (equal); Writing – review & editing (equal).

DATA AVAILABILITY

Data sharing is not applicable to this article as no new data were created or analyzed in this study.

REFERENCES

[1] J. M. Borwein, D. Nuyens, A. Straub, and J. Wan, in *22nd International Conference on Formal Power Series and Algebraic Combinatorics (FPSAC 2010)*, edited by S. Billey and V. Reiner (DMTCS, San Francisco, 2010), pp. 191–202.
[2] J. M. Borwein, D. Nuyens, A. Straub, and J. Wan, Ramanujan J. **26**, 109 (2011).
[3] P. R. Wallace, Phys. Rev. **71**, 622 (1947).
[4] F. H. Burkitt, C. A. Coulson, and H. C. Longuet-Higgins, Trans. Faraday Soc. **47**, 553 (1951).
[5] R. McWeeny, *Coulson's Valence*, *Oxford Chemistry Series* (Oxford University Press, 1979).
[6] P. W. Fowler and B. T. Pickup, J. Chem. Phys. **151**, 151101 (2019).
[7] G. W. Wheland, J. Chem. Phys. **2**, 474 (1934).
[8] M. Bradburn, C. A. Coulson, and G. S. Rushbrooke, Proc. R. Soc. Edinburgh, Sect. A **62**, 336 (1948).
[9] C. A. Coulson and R. Taylor, Proc. Phys. Soc. A **65**, 815 (1952).
[10] J. Barriol and J. Metzger, J. Chim. Phys. **57**, 848 (1960).
[11] K. Pearson, Nature **72**, 294 (1905).
[12] K. Pearson, Nature **72**, 342 (1905).
[13] M. Abramowitz, *Handbook of Mathematical Functions, with Formulas, Graphs, and Mathematical Tables* (Dover Publications, Inc., 1974).
[14] P. W. Fowler and B. T. Pickup, Match Commun. Math. Comput. Chem. **92**, 371 (2024).
[15] R. Taylor and C. A. Coulson, Proc. Phys. Soc. A **65**, 834 (1952).
[16] See https://oeis.org for more information about The on-line encyclopedia of integer sequences, OEIS Foundation Inc. (2026).
[17] J. Hubbard, Proc. R. Soc. London, Ser. A **276**, 238 (1963).
[18] M. Qin, T. Schäfer, S. Andergassen, P. Corboz, and E. Gull, Annu. Rev. Condens. Matter Phys. **13**, 275 (2022).
[19] D. P. Arovas, E. Berg, S. A. Kivelson, and S. Raghu, Annu. Rev. Condens. Matter Phys. **13**, 239 (2022).
[20] R. McWeeny and B. T. Sutcliffe, *Methods of Molecular Quantum Mechanics* (Academic Press, New York, 1969).
[21] M.-H. Zeng, Y.-J. Wang, and T. Ma, Phys. Rev. B **105**, 035155 (2022).
[22] N. Hamada, S.-i. Sawada, and A. Oshiyama, Phys. Rev. Lett. **68**, 1579 (1992).
[23] B. Borštnik and D. Lukman, Chem. Phys. Lett. **228**, 312 (1994).
[24] A. Ceulemans, L. F. Chibotaru, S. A. Bovin, and P. W. Fowler, J. Chem. Phys. **112**, 4271 (2000).
[25] A. H. R. Palser,"Theoretical properties of carbon nanotubes," DPhil thesis (University of Oxford, 2020).
[26] A. H. R. Palser and D. E. Manolopoulos, Phys. Rev. B **58**, 12704 (1998).
[27] A. Rubio, J. L. Corkill, and M. L. Cohen, Phys. Rev. B **49**, 5081 (1994).
[28] N. G. Chopra, R. J. Luyken, K. Cherrey, V. H. Crespi, M. L. Cohen, S. G. Louie, and A. Zettl, Science **269**, 966 (1995).
[29] T. Xu, K. Zhang, Q. Cai, N. Wang, L. Wu, Q. He, H. Wang, Y. Zhang, Y. Xie, Y. Yao, and Y. Chen, Chem. Eng. J. **431**, 134118 (2022).
[30] G. Dresselhaus, M. S. Dresselhaus, and R. Saito, *Physical Properties of Carbon Nanotubes* (Imperial College Press, London, 1998).
[31] C. T. White and J. W. Mintmire, J. Phys. Chem. B **109**, 52 (2005).
[32] D. J. Chadi and M. L. Cohen, Phys. Status Solidi B **68**, 405 (1975).